Doctor of Philosophy

Protective effect of cyclin-dependent kinase inhibitors against oxidative stress-induced neuronal death via inhibition of TRPC5-mediated calcium influx in epilepsy

The Graduate School
of the University of Ulsan

Department of Medicine
Ji Hoon Song

이학박사 학위논문

뇌전증에서 cyclin-dependent kinase 억제제의 산화적 손상에 의해 유도되는 TRPC5 매개 칼슘 이온 유입 억제를 통한 신경 세포 사멸 보호 효과

Protective effect of cyclin-dependent kinase inhibitors against oxidative stress-induced neuronal death via inhibition of TRPC5-mediated calcium influx in epilepsy

울 산 대 학 교 대 학 원

의 학 과

송 지 훈

Protective effect of cyclin-dependent kinase inhibitors against oxidative stress-induced neuronal death via inhibition of TRPC5-mediated calcium influx in epilepsy

Supervisors: Jae-Young Koh
Jung Jin Hwang

A Dissertation

Submitted to
the Graduate School of the University of Ulsan
In Partial Fulfillment of the Requirements
for the Degree of

Doctor of Philosophy in Science

by

Ji Hoon Song

Department of Medicine

Ulsan Korea

August 2018

Protective effect of cyclin-dependent kinase inhibitors against oxidative stress-induced neuronal death via inhibition of TRPC5-mediated calcium influx in epilepsy

This certifies that the dissertation

of Ji Hoon Song is approved.

Committee Vice-chair	Dr. Seok Ho Hong
Committee Member	Dr. Jae-Young Koh
Committee Member	Dr. Jung Jin Hwang
Committee Member	Dr. Joo-Yong Lee
Committee Member	Dr. Dong-Hyung Cho

Department of Medicine

August 2018

Abstract

Background: Epilepsy is one of the most common neurological disorders caused by recurrent spontaneous seizure which lead neuronal death. Neurons are highly vulnerable to oxidative stress that triggers death signaling in acute brain injuries such as seizures and ischemic and traumatic brain injuries. During oxidative insults, intracellular calcium ion (Ca^{2+}) and zinc ion (Zn^{2+}) play critical roles in neuronal death. However, relationship of oxidative stress and these two ions during neuronal death need to be elucidated.

Purpose: The aims of this study are to identify strong neuroprotective molecules against oxidative stress-induced neuronal death and to demonstrate the underlying mechanism for the neuroprotective effect of these drugs.

Results: When the primary cultures containing both cortical neurons and astrocytes were exposed to hydrogen peroxide (H_2O_2), the majority of cells died and increased the release of lactate dehydrogenase (LDH) into the bathing medium. Addition of either NU6027 or indirubin-3'-oxime (I3O) markedly reduced the H_2O_2-induced cell death. The protective effect of NU6027 or I3O was also observed in cells treated with $ZnCl_2$ or sodium nitroprusside (SNP; a donor of nitric oxide). Interestingly, the drugs selectively protected neurons, while they had no effect on astrocytes. When I analyzed Zn^{2+} and Ca^{2+} signals with live cell images of neurons exposed to H_2O_2, early Zn^{2+} rises were a prerequisite for late Ca^{2+} increases. Although both NU6027 and I3O had no effect on Zn^{2+} rises, they dramatically abrogated Ca^{2+} rises. On the other hand, N,N,N′,N′-tetrakis-(2-pyridylmethyl) ethylenediamine (TPEN) blocked both Zn^{2+} and Ca^{2+} rises. To figure out the route of Ca^{2+} responsible for H_2O_2-induced neuronal death, I treated the cells with several inhibitors for receptors and channels which are permeable to Ca^{2+}. The results showed that H_2O_2-induced neuronal death was not attenuated by MK801 [N-methyl-D-aspartate (NMDA) receptor antagonist], 6-cyano-7-nitroquinoxaline-2,3-dione [CNQX; alpha-amino-3-hydroxy-5-methyl-4-isoxaxolepropionic acid (AMPA)/kainic acid

(KA) receptor antagonist], (-)-xestospongin C (inositol trisphosphate receptor antagonist), dantrolene (ryanodine receptor antagonist). Interestingly, 2-aminoethyl diphenylborinate [2-APB; transient receptor potential (TRP) channel blocker] and ML204 (TRPC5 blocker) significantly decreased Ca^{2+} as well as neuronal death induced by H_2O_2, suggesting that TRPC may be involved. I found that TRPC5 was exclusively expressed in neurons, and neurons from TRPC5 knock out (KO) mice were resistant to neuronal death by H_2O_2 compared with wild type (WT) neurons. Additionally, electrophysiological analysis indicated that the NU6027 and I3O directly blocked the basal activity of TRPC5 and Zn^{2+}-mediated TRPC5 activation in human embryonic kidney 293 (HEK293) cells expressing mouse TRPC5 proteins. NU6027 reduced mortality without the effect on seizure severity in KA-induced seizure animal models, in which oxidative stress plays a role in neuronal death. Furthermore, NU6027 significantly attenuated the resultant neuronal death in cerebral cortex and hippocampus of KA-induced seizure rats.

Conclusion: This study suggests that NU6027 and I3O directly block TRPC5 channels which mediate Zn^{2+}-dependent Ca^{2+} influx and oxidative stress-induced neuronal death. Therefore, the inhibition of TRPC5 can be a novel target for developing drugs for epilepsy.

Keyword: Calcium ion, epilepsy, neuronal death, oxidative stress, transient receptor potential canonical 5 (TRPC5), and zinc ion

Contents

List of Tables

List of Figures

Abbreviations

2-APB: 2-aminoethyl diphenylborinate

ACA: anthranilic acid

Amg: amygdala

AMPA: alpha-amino-3-hydroxy-5-methyl-4-isoxaxolepropionic acid

Ca^{2+}: calcium ion

$[Ca^{2+}]_i$: intracellular concentrations of Ca^{2+}

CDK: cyclin dependent kinase

CLT: clotrimazole

CNQX: 6-cyano-7-nitroquinoxaline-2,3-dione

FFA: flufenamic acid

FJB: fluoro-Jade B

GFAP: glial fibrillary acidic protein

GSK3β: glycogen synthase kinase 3β

H_2O_2: hydrogen peroxide

I3O: indirubine-3'-oxime

IP3R: inositol trisphosphate receptors

KO: knockout

LDH: lactate dehydrogenase

NKA: Na^+/K^+-ATPase

NMDA: N-methyl-D-aspartate

NO: nitric oxide

PI: propidium iodide

Pir: piriform cortex

R-GECO1: p-CMV-R-GECO1 plasmid

ROS: reactive oxygen species

RR: ruthenium red

RT-PCR: reverse transcription-polymerase chain reaction

RyR: ryanodine receptors

TPEN: N,N,N,N′-tetrakis (2-pyridylmethyl) ethylenediamine

TRP: transient receptor potential

TRPA: transient receptor potential ankyrin

TRPC: transient receptor potential canonical

TRPM: transient receptor potential melastatin

TRPV: transient receptor potential vanilloid

VDCC: voltage-dependent calcium channels

WT: wild-type

XeC: (-)-xestospongin C

Zn^{2+}: zinc ion

$[Zn^{2+}]_i$: intracellular concentrations of Zn^{2+}

Introduction

Epilepsy is characterized by recurrent unprovoked seizure and the fourth most common neurological disorder. Worldwide, more than 65 million people are distressed with epilepsy and over 100,000 patients are newly diagnosed every year.[1)] Epilepsy is associated with several risk factors, including brain tumors, the developmental abnormalities in brain, traumatic brain injury, and stroke.[2)] Although about 70% of these patients are controlled by currently used antiepileptic drugs, approximately 30% are still refractory. It has been reported that single or repeated seizure induced neuronal loss in the brain, especially in hippocampus. The neuronal death is stimulated by overloaded calcium ion (Ca^{2+}) and oxidative stress. In animal models, the injection of kainic acid (KA) or pilocarpine increases excessive production of reactive oxygen species (ROS) which contributes to neuronal cell death.[3)] Moreover, seizure-induced neuronal death was mediated by Ca^{2+} overload by mitochondrial dysfunction and oxidative stress.[4)]

ROS plays important pathological roles in numerous neurological disorders, such as ischemic stroke, brain and spinal cord trauma, and epilepsy.[3, 5, 6)] ROS includes hydrogen peroxide (H_2O_2), nitric oxide (NO), superoxide anions, and hydroxyl radicals.[7)] The physiological levels of ROS can be maintained by cellular antioxidant detoxification systems, such as superoxide dismutase, catalase, and glutathione peroxidase.[8)] However, excessive ROS by an imbalance between the production of ROS and the ability of detoxification leads cell death.[9)] In particular, neurons are prone to be damaged by oxidative stress because brain contains high level of polyunsaturated fatty acids which are more susceptible to peroxidation, consumes the considerable amount of oxygen even though its relatively small weight, and possesses the limited antioxidant activity compared with other tissues.[10)]

In addition to oxidative stress, the consequent rise of intracellular concentrations of Ca^{2+} ($[Ca^{2+}]_i$) are considered to be principal for neural excitotoxicity in brain injuries such as

epilepsy, stroke, and brain/spinal cord trauma.[3, 5, 6] It has been reported that various receptors and channels including glutamate receptors [N-methyl-D-aspartate (NMDA), alpha-amino-3-hydroxy-5-methyl-4-isoxaxolepropionic acid (AMPA)/KA receptors], voltage-dependent calcium channels (VDCC), transient receptor potential (TRP) channels, inositol trisphosphate receptors (IP3R) and ryanodine receptors (RyR) are involved in the elevation of $[Ca^{2+}]_i$ during neuronal death.[11-13] Particularly, the recent studies suggested that TRP channels, Ca^{2+}-permeable non-selective cationic channels, have implicated in oxidative stress-induced increases in $[Ca^{2+}]_i$.[14, 15]

Mammalian TRP channels are divided into seven subfamilies; TRPC (canonical), TRPM (melastatin), TRPV (vanilloid), TRPA (ankyrin), TRPP (polycystic), TRPML (mucolipin), and TRPN (no mechanoreceptor potential C).[16] The isoforms of TRP channels are consisted of six transmembrane domains, a pore-forming loop between fifth and sixth transmembrane domains, and the intracellular C- and N-termini.[17] They form homo- or hetero-tetramers to form as a channel.[17, 18] Many TRP channels are critical in various neurological functions, such as cell proliferation, dendritic outgrowth, growth corn development, axon guidance, neuroprotection and neuronal death.[16, 17] On the other hand, it has been reported that TRPC channels are implicated in neuronal death, which are consisted of seven isotypes (TRPC1–TRPC7) and highly expressed in the brain.[11, 19] Recent studies reported that TRPC4 and TRPC5 were associated with epileptiform burst firing and seizure-induced neuronal death.[20, 21] Moreover, it was reported that S-glutathionylation of TRPC5 is involved in oxidative stress-mediated neuronal death in Huntington's disease.[15] However, the role of TRPCs on oxidative stress-induced neuronal death has not been clearly investigated.

Besides, zinc ions (Zn^{2+}) also play physiological and pathological roles in the brain. Under physiological conditions, intracellular Zn^{2+} is tightly regulated by zinc transporters (ZnTs), ZRT/IRT-like proteins (ZIPs), and buffering proteins including metallothionein.[22-24] However, the intracellular concentrations of Zn^{2+} $[Zn^{2+}]_i$ are excessively increased during

neuronal death under pathological conditions, such as seizures, stroke, or traumatic brain injury.[25-27] Interestingly, several papers suggested that the two potentially toxic events, Ca^{2+} and Zn^{2+} dyshomeostasis, are closely correlated. Vander Jagt *et al*. reported that increases in intracellular Zn^{2+} contribute to the subsequent Ca^{2+} increase in CA1 pyramidal neurons exposed to NMDA.[28] It has been also demonstrated that increase in intracellular Zn^{2+} by clioquinol and pyrithione, Zn^{2+}-ionophores, can activate TRPA1 in dorsal root ganglion neurons.[29] However, the mechanisms of Zn^{2+}-mediated Ca^{2+} influx during neuronal death has not been clearly demonstrated.

Although ample evidence supports that oxidative stress is a key mechanism contributing to neuronal death in acute brain injury, a variety of clinical trials with drugs targeting ROS have been unsuccessful. For instance, potent antioxidants, such as N-acetyl cysteine and NXY-059, were not beneficial in patients with epilepsy or ischemic stroke.[30, 31] There are many possible reasons for these failures, including weak antioxidant capacity, poor blood–brain barrier penetration, and rapid clearance in vivo.[32] Despite the failure of variety of clinical trials with antioxidant drugs, ROS is still a major target for neuroprotective drugs. Hence further studies are needed to find the novel toxic mechanism of oxidative insults.

In the present study, I found that two cyclin dependent kinase (CDK) inhibitors, NU6027 and indirubine-3'-oxime (I3O), efficiently prevented Zn^{2+}-mediated Ca^{2+} increases and neuronal death induced by ROS. I focused on finding a rout of the Ca^{2+} overload, evaluating whether the rout can be a target for NU6027 and I3O, and efficacy of NU6027 in zinc transporter-induced rat seizure models.

Materials and Methods

Primary cortical cell cultures

Cortices of postnatal day 3 ICR mouse brains were collected and used to prepared pure astrocyte cultures. The pure astrocyte cultures were maintained in Dulbecco's modified Eagle's medium (DMEM; Gibco, Grand Island, NY, USA) supplemented with 7% fetal bovine serum (FBS; Hyclone, Logan, UT, USA), 7% horse serum (HS; Gibco), 1% penicillin/streptomycin (Cambrex, Walkersville, MD, USA), and freshly added 2 mM glutamine (Sigma, St. Louis, MO) until forming monolayer. These astrocyte cultures were used either for experiments or as feeder cells for mixed cortical cultures. For mixed cortical cultures, cortical neurons from cortices of embryonic day 14 (E14) ICR mouse brains were plated onto each plate containing pure astrocyte cultures and growing them in DMEM containing 5% FBS, 5% HS, 1% penicillin/streptomycin, and freshly added 2 mM glutamine. Pure neuronal cultures were prepared from cortices of E14 ICR mice or age-matched WT or TRPC5 KO 129/SvImJ mice. Neurons were grown in neurobasal media (Gibco) containing B27 supplement (Gibco), 2 mM glutamine and antibiotics. Cytosine arabinoside (Sigma) was added to mixed cortical cultures and pure neuronal cultures to eliminate non-neuronal cells. All cultures were maintained at 37℃ in a humidified 5% CO_2 incubator and replaced with appreciated culture media twice a week.

Treatments

Cells were treated with glutamate (Sigma), hydrogen peroxide (H_2O_2; Sigma), sodium nitroprusside (SNP; Sigma), and $ZnCl_2$ in Minimum Essential Media (MEM; Gibco) for 24 h at the concentrations. Anthranilic acid (AA), clotrimazole (CLT), dantrolene, flufenamic acid (FFA), indirubin-3′-oxime (I3O), NU6027, ruthenium red (RR), N,N,N,N′-tetrakis (2-pyridylmethyl) ethylenediamine (TPEN) and 2-aminoethyl diphenylborinate (2-

APB) were purchased from Sigma. Capsaicin, MK-801, ML204, Pyr3 and (-)-xestospongin C (XeC) were purchased from Tocris (San Diego, CA, USA). SB216763 was purchased from Enzo Life Science (Farmingdale, NY, USA). 6-cyano-7-nitroquinoxaline-2,3-dione (CNQX) was purchased from RBI (Natick, MA, USA). All these reagents were added 1 h prior to H_2O_2, $ZnCl_2$, or SNP exposure, unless otherwise stated.

Determination of cell death

To evaluate cell death, the release of lactate dehydrogenase (LDH) into culture media from dead cells was measured after the exposure to H_2O_2, $ZnCl_2$, SNP, or glutamate for 24 h. Cell death was quantitatively assessed. Each LDH value was subtracted by the mean background values in sham washed control (0%; without cell death) followed by scale to the mean value in sister cultures treated with 200 μM glutamate (100%; near-complete neuronal death) or 100 μM $ZnCl_2$ (100%; astrocytic death) in neuron cultures or pure astrocyte cultures, respectively. Cell death was also determined by staining cells with 2 μg/ml propidium iodide (PI) to identify the disruption of membrane integrity indicating cell death. Phase-contrast and fluorescent images were obtained using a fluorescence microscope (IX71; Olympus, Tokyo, Japan) equipped a CCD camera (IX-10, Olympus). Fluorescent images for PI-stained cells were obtained at the excitation wavelength of 535 nm and emission wavelength of 617 nm.

Live cell imaging for intracellular Ca^{2+} and Zn^{2+}

To stain cells for Ca^{2+} and label Zn^{2+}, mixed cortical cultures were stained with 2 μM Fluo-4 AM (a chemical indicator for Ca^{2+}) or 2.5 μM FluoZin-3 AM (a chemical indicator for Zn^{2+}) in phenol red free MEM for 30 min before imaging. Fluorescent images of Fluo-4 or FluoZin-3 were obtained suing a fluorescence microscope (IX71; Olympus) equipped with CCD camera (IX-10; Olympus) at the excitation wavelength of 494 nm and emission wavelength of 516 nm. Fluorescence intensities were quantified in each captured field using

ImageJ software (National Institute of Health) and represented by fold increase compared with control. Additionally, time laps live-cell imaging, pure neuron cultures were loaded with 2.5 μM FluoZin-3-AM to label Zn^{2+} for 30 min before imaging or transfected 2 days before imaging with 10 μg of p-CMV-R-GECO1 plasmid (R-GECO1; 565/630 nm of excitation/emission wave length; genetically encoded Ca^{2+} indicating protein) to detect Ca^{2+}. After the addition of H_2O_2, images were acquired every 1 min for 4 h using the inverted microscope (Ti-E; Nikon) equipped with a Cascade 212B (EMCCD) camera (Roper Scientific, Trenton, NJ, USA) at an appropriate excitation and emission wavelength. Fluorescent intensity was analyzed with MetaMorph software (Universal imaging, Downingtown, PA, USA) and represented by fold increases compare with control.

Reverse transcription-polymerase chain reaction (RT-PCR)

Total cellular RNA was extracted from pure neuron and astrocyte cultures using Trizol (Invitrogen) according to manufacturer's instruction. Complementary DNA (cDNA) was synthesized using RT^2 First Strand kit (Qiagen, Limburg, Netherlands). PCR reaction were prepared by mixing equal amount of cDNA and a set of primers for mouse TRPC subtypes (Table 1) in AccuPower ProFi Taq PCR premix (BioNeer, Daejeon, South Korea) and completed with C1000 Thermal Cycler (Bio-Rad, Hercules, CA, USA) (Table 1). PCR products were separated on 1.5% agarose gels and visualized using Gel-doc (Bio-Rad).

Immunocytochemical staining

Cultured pure neurons and astrocytes were fixed with 4% paraformaldehyde for 15 min and permeabilized with 0.1% Triton X-100 for 5 min. Tissues were then blocked with 1% bovine serum albumin for 30 min. For staining, cells were incubated with antibody for TRPC5 (1:100; Neuromab, Davis, CA, USA) at 4°C overnight followed by incubation for 2 h with glial fibrillary acidic protein (GFAP; 1:100; Millipore, Billerica, MA, USA) for astrocyte or

microtubule-associated protein 2 (MAP2; 1:100; Abcam) for neurons. Cells were then incubated with the appropriate fluorescence-labeled secondary antibodies for 2 h. For nuclear staining, cells were incubated with 5 mg/ml hoechst33342 (Sigma). Cells were mounted and visualized under the EVOS Cell Imaging System (Thermo Fisher Scientific, Rockford, IL, USA).

Western blot analysis

To extract the membrane proteins, the cultured pure neurons and astrocytes were harvested and suspended with 1 mM sodium bicarbonate buffer containing proteinase inhibitors. Membrane pellets were collected by centrifugation at 4℃ and 12,000 rpm for 20 min and resuspended in RIPA buffer (20 mM Tris-HCl pH 7.4, 150 mM NaCl, 1 mM EDTA, 0.5% SDS, 2.5 mM sodium pyrophosphate, 1 μM Na_3VO_4, and protease inhibitors). The same amount of membrane proteins was separated by 8 % SDS-PAGE and electrically transferred to polyvinylidene difluoride membranes (Millipore). The membranes incubated overnight at 4℃ with primary antibodies for TRPC5 (1:200) and Na^+/K^+ ATPase (NKA; 1:3,000; Sigma). Subsequently, the membrane was probed with horseradish peroxidase-conjugated anti-mouse IgG (1:1,000) or anti-rabbit IgG (1:2,000) secondary antibodies (Thermo Fisher Scientific). Immunoreactive bands were visualized using Immunobilon Western Chemiluminescent HRP Substrate (Millipore) and the Kodak Image Station 4000MM (Kodak).

Electrophysiological analysis

For TRPC5 current recordings, human embryonic kidney (HEK) 293 cells (ATCC) were maintained according to the manufacturer's recommendations and transfected with plasmid DNA expressing mouse TPRC5 (pIRES-mTRPC5-GFP) using FuGENE6 (Roche, Indianapolis, IH, USA). Whole cell currents were recorded using an Axopatch 200B amplifier (Axon Instruments). Currents were filtered at 5 kHz (3 dB, 4-pole Bessel), digitized using a

Digidata 1440A Interface (Axon Instruments), and analyzed using a personal computer equipped with pClamp 10.2 software (Axon Instruments) and Origin software (Microcal Origin v. 8.0). Patch pipettes were made from borosilicate glass and had resistances of 2–4 MΩ when filled with standard intracellular solutions. An external bath medium (normal Tyrode solution; as the following composition: 135 mM NaCl, 5 mM KCl, 2 mM $CaCl_2$, 1 mM $MgCl_2$, 10 mM glucose, and 10 mM N-[2-hydroxyethyl]piperazine-N-[2-ethanesulfonic acid] (HEPES), at pH 7.4 adjusted with NaOH) were used. A Cs^+-rich external solution was made by replacing NaCl and KCl with equimolar CsCl. The standard pipette solution contained 140 mM CsCl, 10 mM HEPES, 0.2 mM Tris-GTP, 0.5 mM EGTA, and 3 mM Mg-ATP, at the pH 7.3 adjusted with CsOH. After TRPC5 activation in a Cs^+-rich solution, 10 μM NU6027 or 10 μM I3O was externally applied at the time indicated by the bars. $ZnCl_2$ was intracellularly applied via the pipette solution. Voltage ramp pulses were applied from +100 to −100 mV for 500 ms at a holding potential of −60 mV. The junction potential between the pipette and bath solutions used for all cells during sealing was calculated to be 5 mV (pipette negative) using pClamp 10.2 software. No junction potential correction was applied. Experiments were performed at room temperature (18°C–22°C). Cells were continuously perfused at a rate of 0.5 ml/min. The inward current amplitudes of all bar graphs and current traces were taken during the ramp pulses at a holding potential of −60 mV.

Genotyping for pure neuronal cultures from WT and TRPC5 KO mice

E14 WT and TRPC5 knockout (KO) littermates in a mixed genetic background (129/SvImJ:C57BL/6) were used to establish pure neuron cultures. To determine the genotype of pure neuron cultures, total genomic DNA was isolated from the brain tissues of WT and TRPC5 KO mice using DNA extraction buffer (50 mM Tris –HCl, pH 8.0, 100 mM EDTA, 0.5% SDS, and a freshly added 0.2 mg/ml proteinase K). PCR reaction were prepared by mixing 200 ng of mouse tail DNA and a set of primers (Table 2) in AccuPower ProFi Taq PCR

premix (BioNeer) and completed using C1000 Thermal Cycler. PCR products were resolved on 1 % agarose gel and visualized using Gel-doc (Bio-Rad).

Animals

The animal experiment protocol was approved by the Internal Review Board for Animal Experiments of Asan Life Science Institute, University of Ulsan College of Medicine. Eight-week-old male Sprague-Dawley (SD) rats (240–270g) were used for all animal experiments. Animals were allowed to freely access to food and water and maintained under 12 h light/12 h dark cycles.

Animal model of KA-induced seizure

For induction of seizure, animals were intraperitoneally injected with 10 mg/kg of KA (Tocris Bioscience, Bristol, UK) dissolved in normal saline. To identify the neuroprotective effect of NU6027, 100 μg/kg NU6027 or 10% DMSO in saline as a vehicle were injected 30 min after KA injection. To halt seizures, animals were intraperitoneally injected with 50 mg/kg sodium phenytoin two and half hours after the seizure induction. The animals were continuously monitored for 2 h following injection with KA and classified into 5 stages of seizure severity using the classification system developed by Zhang et al..[33)]

Tissue preparation and histological staining

Twenty-four hours after KA injection, body weight and mortality of animals were determined, and brains were collected from the animal and frozen in immediately. The brains were then cut in 10 μm thickness using cryostat (CM3050; Leica) and mounted on poly-L-lysine coated slide glasses. To verify the neuronal loss and death, the brain sections on the slide were fixed with 4% paraformaldehyde and then stained with 1% cresyl violet or 0.001% Fluoro-Jade B (FJB) solution (Histo-Chem Inc., Jefferson, AR, USA). All Images were

obtained with a fluorescence microscope (BX60; Olympus) equipped with DP70 CCD camera (Olympus). The numbers of FJB-positive neurons in each brain regions including hippocampus and cortex were counted in 5 coronal sections which were 100 μm thick apart starting 3.3 mm from the bregma.

Statistical analysis

All experimental data collected from more than three individual experiments and represented as the mean ± SEM. Statistical significances were evaluated by two-tailed Student's t-test for the comparisons between two groups and One-way ANOVA test for the comparisons of multiple groups. A p-value of <0.05 was considered statistically significant.

Table 1. List of primers used for RT-PCR

Genes	Forward primers (5'->3')	Reverse primers (5'->3')	Accession number
TRPC1	TGGGATGATTTGGTCAGACA	CCAATGAACGAGTGGAAGGT	NM_011643
TRPC2	AGCCTCAGTACATTGCCCTG	AAGTTCCACCAGTCCAGGAG	NM_011644
TRPC3	AGAGCGATCTGAGCGAAGTC	TTTGGAACGAGCAAACTTCC	NM_019510
TRPC4	ACGCGTTTTCCACGTTATTC	CTTCGGTTTTTGCCTCTCTG	NM_016984
TRPC5	ATTATTCCCAGCCCCAAATC	GACAGGCCTTTTTCTTGCAG	NN_009428
TRPC6	AAAGATATCTTCAAATTCATGGTC	CACGTCCGCATCATCCTCAATTTC	NM_013838
TRPC7	CGTGCTGTATGGGGTTTATAATG	GCTTTGGAATGCTGTTAGAC	NM_012035
Actin	TGTTACCAACTGGGACGACA	AAGGAAGGCTGGAAAAGAGC	NM_007393

Table 2. List of primers used for genotyping WT and TRPC5 KO neuronal cultures

Genes	Forward primers (5'->3')	Reverse primers (5'->3')
TRPC5 WT	GTAAGTGATACTAGGTATGGGGTATGGAGG	CACCAATCATGGATGTATTCCGTG
TRPC5 KO	GTAAGTGATACTAGGTATGGGGTATGGAGG	GTCGACACACGTATAAGGCATACTCTTG

Results

CDK inhibitors prevent H_2O_2-induced neuronal death

The present study initially explored the neuroprotective drugs and found two CDK inhibitors, NU6027 and I3O which were effective on oxidative stress-induced cell death (Fig. 1). To investigate the neuroprotective effects of NU6027 and I3O, primary mixed cortical cultures were pretreated with indicated concentrations of NU6027 and I3O for 1 h and then incubated with 150 μM H_2O_2 for 24 h. The treatment of mixed cortical cultures with H_2O_2 markedly increased the release of LDH, a useful biochemical marker to quantify the cell death, while the presence of NU6027 and I3O significantly reduced H_2O_2-induced release of LDH (Fig. 2A). Neuronal cell death, furthermore, was assessed via staining the cells with PI. The results showed that NU6027 and I3O markedly reduced neuronal death induced by H_2O_2 (Fig. 2B). It has been known that many CDK inhibitors including I3O also block glycogen synthase kinase 3β (GSK3β), and GSK3β inhibitors prevent the excitotoxicity in neurons.[34, 35] However, the results indicated that SB216763, a GSK3β-specific inhibitor, did not prevent H_2O_2-induced cell death in mixed cortical cultures (Fig. 2A). These data suggest that the protective effects of NU6027 and I3O against oxidative stress were not associated with inhibition of GSK3β.

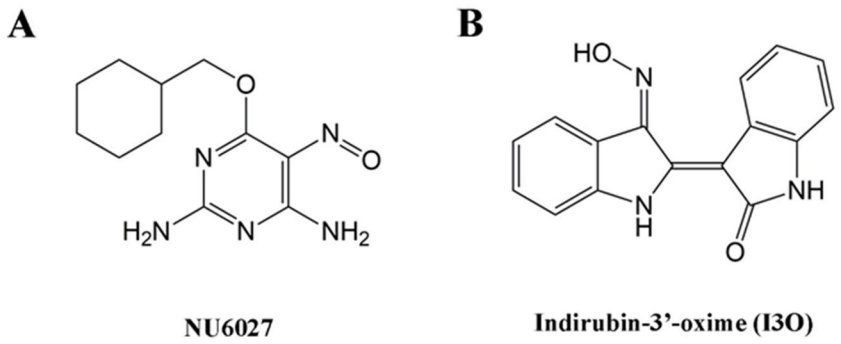

Fig. 1. Chemical structures of NU6027 and indirubin-3'-oxime (I3O).

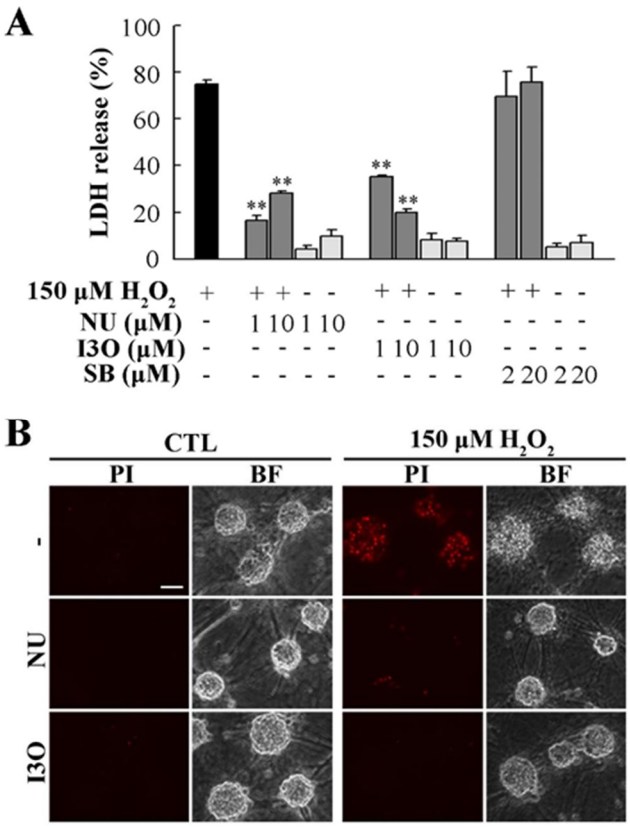

Fig. 2. NU6027 and I3O reduced H_2O_2-induced cell death in mixed cortical cultures. (A) The bars denote the percentage of LDH released from mixed cortical cultures containing neurons and astrocytes 24 h after treatment with 150 μM H_2O_2. The indicated concentrations of NU, I3O, or SB216763 were added 1 h before exposure to H_2O_2 (mean ± SEM, n = 3; ** $p < 0.001$ compared with H_2O_2). (B) Cells were stained with 2 μg/ml PI for 10 min, and bright field (BF) and fluorescent images were obtained using a fluorescent microscope. Scale bar, 50 μm.

NU6027 and I3O prevent oxidative stress-induced neuronal death

The mixed cortical cultures were treated various oxidative stress inducers including SNP as the NO donor and $ZnCl_2$ to determine whether NU6027 and I3O are effective on prevention of cell death induced by oxidative insults. The results showed that both NU6027 and I3O significantly diminished the release of LDH induced by SNP (Fig. 3A). As shown in Fig. 3B, PI-positive cells in mixed cortical cultures treated with SNP were observed in neurons and it was markedly decreased by the treatment with NU6027 and I3O (Fig. 3B). However, NU6027 and I3O partially blocked Zn^{2+}-induced the release of LDH (Fig. 3C). Based on the result of PI-staining, PI-positive cells after the treatment with $ZnCl_2$ in mixed cortical cultures were observed in both neurons and astrocytes, whereas it was diminished by NU6027 and I3O only in neuron, not in astrocytes (Fig. 3D). Although the excessive Zn^{2+} can induce cell death not only in neurons but also in astrocytes, it is highly possible that NU6027 and I3O specifically protect neurons from Zn^{2+}-induced toxicity. To verify whether NU6027 and I3O specifically protect neurons against Zn^{2+}-induced oxidative insults, pure neuronal cultures and pure astrocyte cultures were exposed to $ZnCl_2$ for 24h after the pre-incubation with NU6027 and I3O for 1 h. In the results, NU6027 and I3O significantly reduced the release of LDH increased by Zn^{2+} in pure neuron cultures (Fig 3E). By contrast, NU6027 and I3O did not decrease the Zn^{2+}-induced LDH release in pure astrocyte cultures (Fig. 3F). These results suggest that the protective effect of NU6027 and I3O against oxidative stress induced by various mediators is specific in neurons.

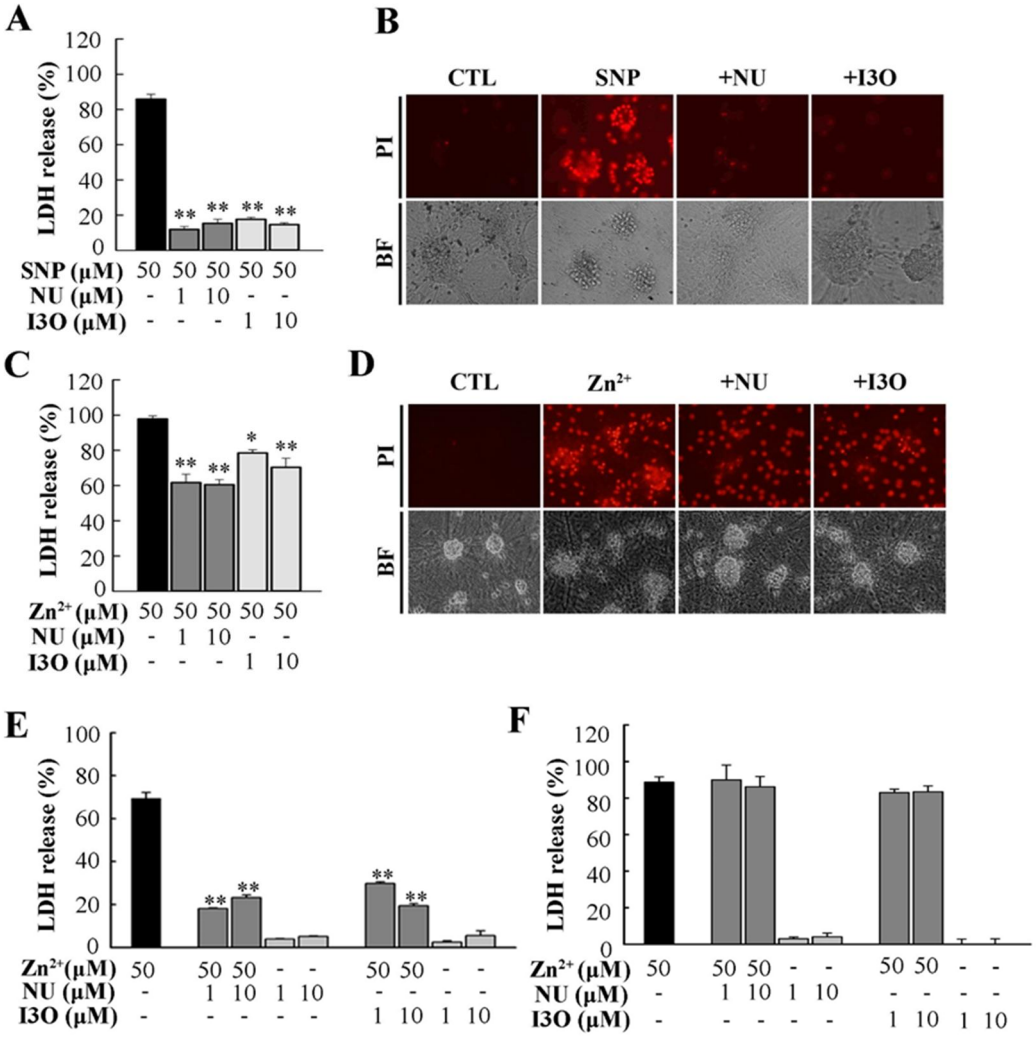
A
LDH release (%)
120
100
80
60
40
20
0
**
SNP (μM) 50 50 50 50 50
NU (μM) - 1 10 - -
I3O (μM) - - - 1 10
B
CTL
SNP
+NU
+I3O
PI
BF
C
LDH release (%)
*
Zn2+ (μM) 50 50 50 50 50
NU (μM) - 1 10 - -
I3O (μM) - - - 1 10
D
CTL
Zn2+
+NU
+I3O
PI
BF
E
LDH release (%)
Zn2+ (μM) 50 50 50 - - 50 50 - -
NU (μM) - 1 10 1 10 - - - -
I3O (μM) - - - - - 1 10 1 10
F
LDH release (%)
Zn2+ (μM) 50 50 50 - - 50 50 - -
NU (μM) - 1 10 1 10 - - - -
I3O (μM) - - - - - 1 10 1 10

Fig. 3. NU6027 and I3O prevented cell death induced by other oxidative stress mediators specifically in neurons. (A) The bars denote the percentage of LDH released from mixed cortical cultures exposed to 50 μM sodium nitroprusside-50 (SNP) for 24 h with or without the indicated concentrations of NU or I3O (mean ± SEM, n = 3; * indicates $p < 0.05$, and ** indicates $p < 0.001$ compared with SNP). (B) Cells were stained with 2 μg/ml PI for 10 min, and bright field (BF) and fluorescent images were obtained using a fluorescent microscope. Scale bar, 50 μm. (C) The bars denote the percentage of LDH released from mixed cortical cultures exposed to 50 μM ZnCl2 (Zn^{2+}) for 24 h with or without the indicated concentrations of NU or I3O (mean ± SEM, n = 3; * indicates $p < 0.05$, and ** indicates $p < 0.001$ compared with Zn^{2+}). (D) Cells were stained with 2 μg/ml PI for 10 min, and bright field (BF) and fluorescent images were obtained using a fluorescent microscope. Scale bar, 50 μm. (E) The bars denote the percentage of LDH released from pure neuronal cultures exposed to 50 μM Zn^{2+} for 24 h with or without the indicated concentrations of NU or I3O (mean ± SEM, n = 3; ** indicates $p < 0.001$ compared with Zn^{2+}). (F) The bars denote the percentage of LDH released from pure astrocyte cultures exposed to 50 μM Zn^{2+} for 24 h with or without the indicated concentrations of NU or I3O (mean ± SEM, n = 3).

The elevation of Zn^{2+} precedes Ca^{2+} overload by H_2O_2

The levels of intracellular Zn^{2+} and Ca^{2+} were increased during oxidative stress, and these ions play critical roles in oxidative cell death. In this study, therefore, the changes in the levels of these ions by H_2O_2 were analyzed in pure neurons loaded with FluoZin-3 AM or transfected with RGECO1. The results of time lapse recording showed that $[Zn^{2+}]_i$ reached maximal levels in 30 min after the addition of H_2O_2 and gradually return to basal levels while $[Ca^{2+}]_i$ was began to increase 1 h after H_2O_2 treatment and sustained at the maximal levels from 2 to 4 h (Fig. 4). These data indicate that the treatment with H_2O_2 stimulate the increase in $[Zn^{2+}]_i$ prior to increase in $[Ca^{2+}]_i$.

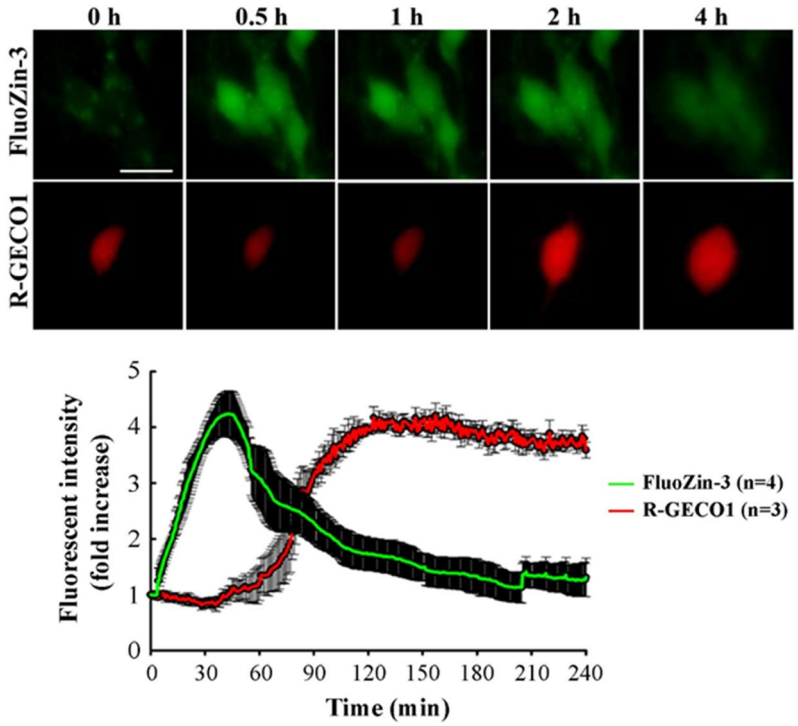

Fig. 4. H_2O_2 triggered early increases in Zn^{2+} prior to Ca^{2+} increases. Pure neuronal cultures were loaded with 2.5 μM FluoZin-3 AM (a chemical indicator for Zn^{2+}) for 30 min or transfected with R-GECO1 (a genetically encoded Ca^{2+} indicating protein) 2 days before experiments. The cells were exposed to 25 μM H_2O_2 and monitored every 1 min for 4 h. Scale bar, 20 μm. The line graph represents the normalized fluorescence intensity of FluoZin-3 and R-GECO1 (mean ± SEM, n = 3 for FluoZin-3, n = 4 for R-GECO1).

NU6027 and I3O specifically block increase in $[Ca^{2+}]_i$ by H_2O_2

To assess the effects of NU6027 and I3O on H_2O_2-triggered elevation of $[Zn^{2+}]_i$ or $[Ca^{2+}]_i$, the mixed cortical cultures were treated with 150 μM H_2O_2 in the presence or absence of 1 μM NU6027, 10 μM I3O, or 1 μM TPEN and stained with 2.5 μM FluoZin-3 AM or Fluo-4 AM for determining $[Zn^{2+}]_i$ or $[Ca^{2+}]_I$, respectively. The results showed that $[Zn^{2+}]_i$ was significantly increased 30 min after exposure to H_2O_2 (Fig. 5A) while the treatment with TPEN almost completely blocked the increased in $[Zn^{2+}]_i$ after exposure to H_2O_2. However, NU6027 and I3O did not inhibit the increase in $[Zn^{2+}]_i$ induced by H_2O_2 (Fig. 5A). By contrast, $[Ca^{2+}]_i$ were significantly increased by H_2O_2 for 2 h in mixed cortical, which were effectively inhibited by NU6027 and I3O (Fig. 5B). Interestingly, pre- and co-treatment with TPEN significantly reduced the elevation of $[Ca^{2+}]_i$ by H_2O_2 while post-treatment with TPEN after the peak of $[Zn^{2+}]_i$ by H_2O_2 did not block further increase in $[Ca^{2+}]_i$ (Fig. 5B). These results indicate that later increase in $[Ca^{2+}]_i$ may be triggered by early Zn^{2+} entry in H_2O_2-treated cells and addition of NU6027 and I3O only block H_2O_2-triggered increase in $[Ca^{2+}]_i$.

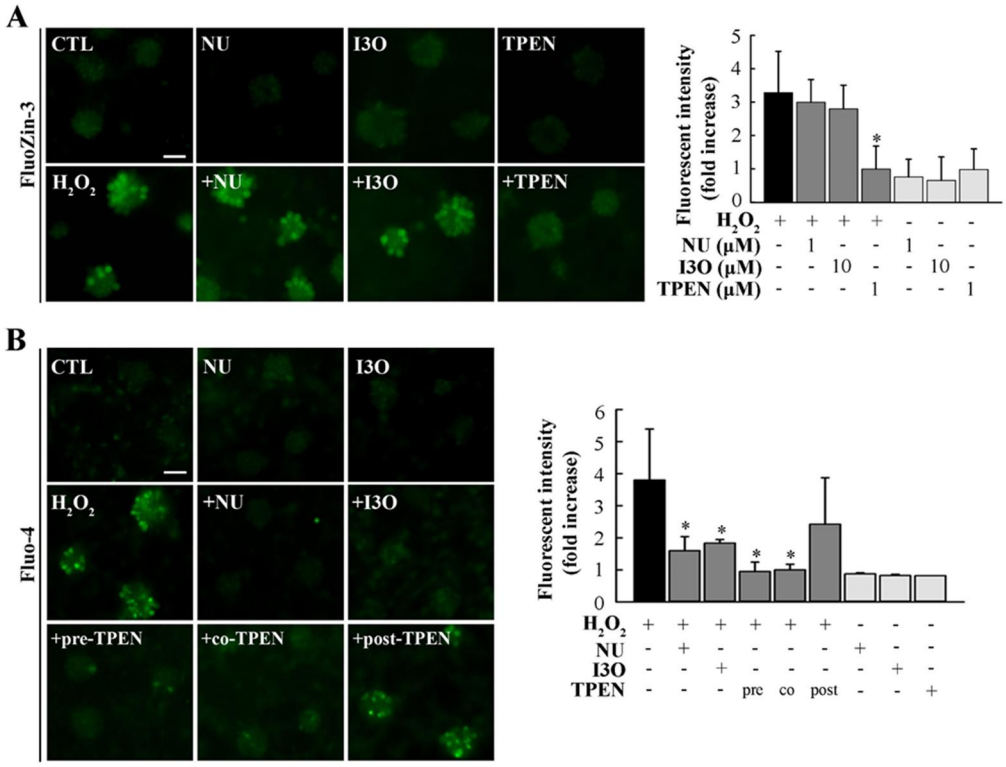

Fig. 5. NU6027 and I3O blocked a delayed Ca^{2+} influx induced by H_2O_2-triggered early increases in Zn^{2+}. (A) Mixed cortical cultures were pretreated with 1 μM NU6027, 10 μM I3O, or 1 μM TPEN 1 h before exposure to 150 μM H_2O_2 for 30 min and then observed under a fluorescent microscope. Cells were stained with 2.5 μM FluoZin-3 AM for 30 min before observation. Scale bar, 50 μm. The bar graph indicates the normalized fluorescence intensity of FluoZin-3 (mean ± SEM, n = 3; * indicates $p < 0.05$ compared with H_2O_2). (B) Mixed cortical cultures were exposed to 150 μM H_2O_2 for 2 h with 1 μM NU6027 or 10 μM I3O 1 h before exposure to 150 μM H_2O_2 for 2 h (middle panel) or the cells were exposed to 150 μM H_2O_2 for 2 h with 1 h pretreatment, cotreatment, or 1 h post-treatment with 1 μM TPEN. Cells were stained with 2 μM Fluo-4 AM for 30 min prior to imaging. Scale bar, 50 μm. The bar graph (right) represents the normalized fluorescence intensity of Fluo-4 (mean ± SEM, n= 3; * indicates $p < 0.05$ compared with H_2O_2).

TRP channels are involved in H_2O_2-induced Ca^{2+} influx

To identify a possible receptors or channels which may contribute to the Ca^{2+} influx triggered by H_2O_2, the mixed cortical cultures were pretreated with various antagonists including 2-APB, CNQX (an antagonist for AMPA/KA receptors), MK801 (an antagonist for NMDA receptors), dantrolene (an antagonist for ryanodine receptors), or (-)-xestosphongin C (antagonist for IP3 receptors) for 1 h and then exposed to H_2O_2 for 24 h additionally. The results indicated that 2-APB significantly reduced H_2O_2-induced release of LDH while others did not (Fig. 6A). Moreover, 2-APB significantly blocked the elevation of $[Ca^{2+}]_i$ triggered by H_2O_2 (Fig. 6B). These results suggest that TRP channels may be important in Ca^{2+} influx triggered by H_2O_2.

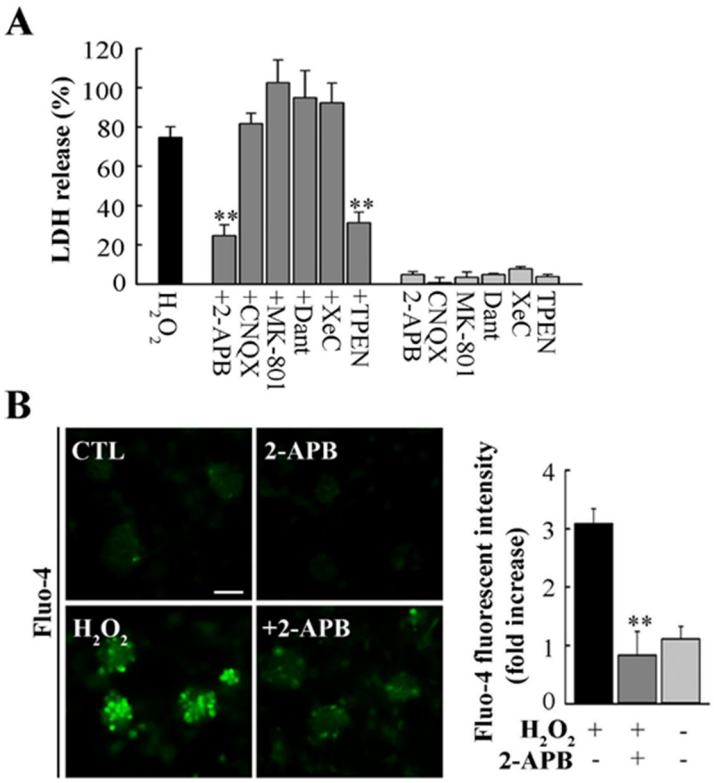

Fig. 6. TRP channels contributed to H_2O_2-triggered neuronal cell death and increase in $[Ca^{2+}]_i$. (A) The bars denote the percentage of LDH released from mixed cortical cultures exposed to 150 μM H_2O_2 for 24 h with or without 50 μM 2-APB, 10 μM CNQX, 10 μM MK-801, 10 μM Dant, 10 μM Xes-C, or 1 μM TPEN (mean ± SEM, n = 3; ** indicates $p < 0.001$ compared with H_2O_2). (B) Mixed cortical cultures were exposed to 150 μM H_2O_2 for 2 h with or without 50 μM 2-APB and stained with 2 μM Fluo-4 AM for 30 min prior to observation. Scale bar, 50 μm. The bar graph represents the normalized fluorescence intensity of Fluo-4 (mean ± SEM, n = 3; ** indicates $p < 0.001$ compared with H_2O_2).

TRPC4 and TRPC5 contribute to the H_2O_2-induced Ca^{2+} influx

Previously, many studies reported that three major subfamilies including TRPC, TRPM, and TRPV were contributed to oxidative stress-induced neuronal death in many neurological diseases. Therefore, this study focused on the potential protective effects of inhibitors against TRPM, and TRPV. However, the results showed that AA, FFA, and CLT (TRPM inhibitors) or RR (a TRPV inhibitor) did not prevent H_2O_2-induced LDH release in mixed cortical cultures (Fig. 7A and B). Moreover, NU6027 and I3O did not block capsaicin-induced LDH release as well as increases in $[Ca^{2+}]_i$ (Fig. 7C and D). These data illustrate that TRPM and TRPV channels are not critical for the present effects. Therefore the study focused on TRPCs against H_2O_2-induced neuronal death and increase in $[Ca^{2+}]_i$. The treatment with ML204, a blocker for TRPC4 and TRPC5, decreased LDH release increased by H_2O_2, whereas Pyr3, a specific blocker for TRPC3, had no effect (Fig. 8A). In consistent with these results, the treatment with ML204 significantly blocked the increase in $[Ca^{2+}]_i$ by the treatment with H_2O_2 while Pyr3 did not (Fig. 8B) . Thus, these data suggest that the TRPC5 are candidates mediating the neuronal cell death and Ca^{2+} influx.

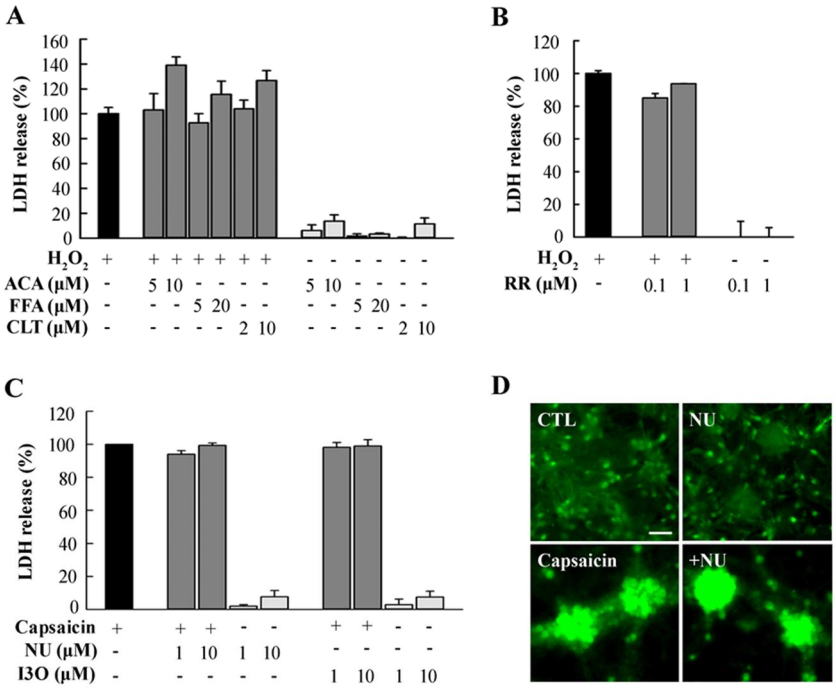

Fig. 7. TRPM or TRPV channels were not responsible for H_2O_2-induced neuronal death. (A) The bars denote percentage of LDH release from the mixed cortical cultures exposed to H_2O_2 with or without anthranilic acid (ACA), flufenamic acid (FFA), clotrimazole (CLT) (mean ± SEM, n=3). (B) The bars denote percentage of LDH release from the mixed cortical cultures exposed to capsaicin with or without Ruthenium red (RR) (mean ± SEM, n=3). (C) The bars denote percentage of LDH release from the mixed cortical cultures exposed to capsaicin with or without 1 μM NU6027 or 10 μM I3O (mean ± SEM, n = 3). (D) Mixed cortical cultures were exposed to 300 μM capsaicin for 3 h with or without 1 μM NU6027 and stained with Fluo-4 AM 30 min before imaging. Scale bar, 50 μm.

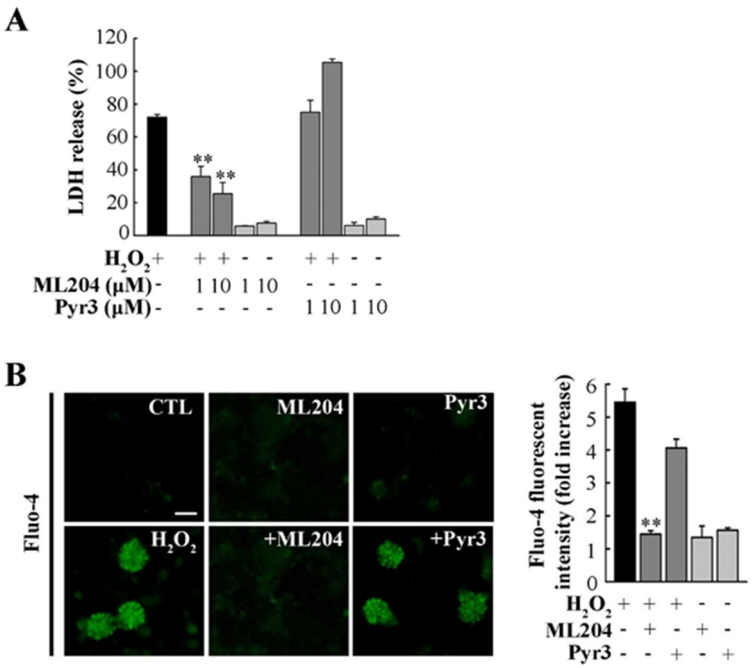

Fig. 8. TRPC4 and TRPC5 were implicated to H_2O_2-induced neuronal death. (A) Mixed cortical cultures exposed to 150 μM H_2O_2 with or without the indicated concentrations of ML204 or Pyr3. Bars denote the percentage of LDH release (mean ± SEM, n = 3; ** indicates $p < 0.001$ compared with H_2O_2). (B) Mixed cortical cultures were exposed to 150 μM H_2O_2 for 2 h with or without 1 μM ML204 or 1 μM Pyr3 and stained with 2 μM Fluo-4 AM. The representative images of Fluo-4 were obtained using a fluorescent microscope. Scale bar, 50 μm. The bar graph represents the normalized fluorescence intensity of Fluo-4 (mean ± SEM, n = 4; ** indicates $p < 0.001$ compared with H_2O_2).

TRPC5 is expressed in neurons

To identify the expression of TRPC isotypes in neurons and astrocytes, RT-PCR was performed using the specific primer sets (Table 2). The results showed that TRPC5 was predominantly expressed in neurons while other isotypes were either expressed in both neurons and astrocytes or not expressed (Fig. 9A). To confirm the neuron-specific expression of TRPC5 proteins, immunocytochemical staining and western blot analysis was carried out for the detection of TRPC5 protein extraction in both neuron and astrocytes. In consistent with RT-PCR, the results of immunohistochemical staining showed that the expression of TRPC5 proteins were expressed only in cultured neurons (Fig 9B). Furthermore, western blotting data also showed that TRPC5 proteins were detectable in only neurons, not in astrocytes (Fig. 9C). These data indicate that TRPC5 is a neuron-specific TRPC isotype and can be a potential rout for the Ca^{2+} influx induced by oxidative stress in neurons.

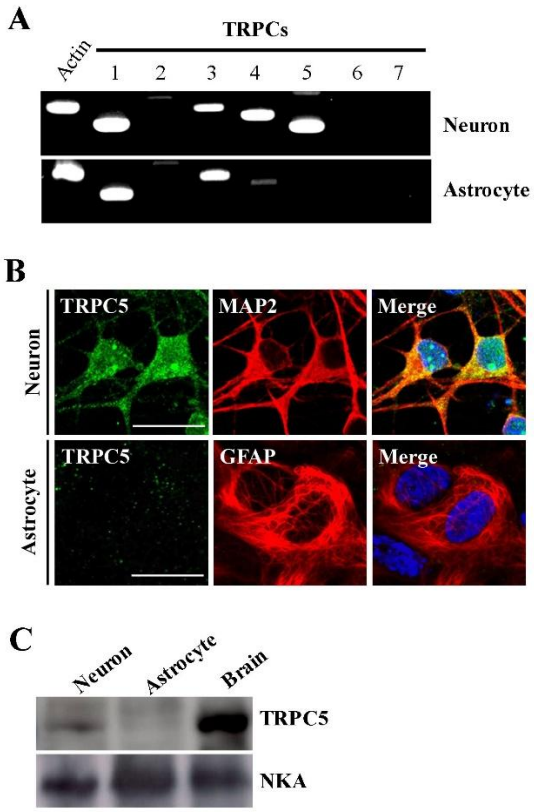

Fig. 9. TRPC5 exclusively expressed in neurons. (A) The expression of TRPC1-7 mRNA was analyzed by RT-PCR using specific primers in pure neuronal and astrocyte cultures. Actin was used as a housekeeping gene. (B) Immunofluorescence images of neurons (upper panel) and astrocytes (lower panel) labeled with TRPC5 antibodies (green) and microtubule-associated protein 2 (MAP2; a marker for neuron; red color) or glial fibrillary acidic protein (GFAP; a marker for astrocyte; red color). Scale bar, 20 μm. (C) The expression of TRPC5 proteins was confirmed by western blot analysis using TRPC5 in membrane fractions purified from pure neuronal and astrocyte cultures. Membrane fractions extracted from mouse whole brain tissue were used as a positive control. Na^+/K^+-ATPase (NKA) were used as a loading control.

TRPC5 is associated with H_2O_2-induced neuronal death and Ca^{2+} influx

Next, the implication of TRPC5 on H_2O_2-induced neuronal death and increase in $[Ca^{2+}]_i$ was elucidated using pure neuron culture from wild-type (WT) and TRPC5 knockout (KO) mice (Fig. 10A). The results showed that H_2O_2 did not induced LDH release in neurons from TRPC5 KO mice (Fig. 10B). It indicates that neurons from TRPC5 KO mice were less sensitive to H_2O_2 toxicity than those from WT mice. Consistent with this result, the exposure to H_2O_2 increased $[Ca^{2+}]_i$ in neurons from WT mice (Fig. 10C). However, $[Ca^{2+}]_i$ was not increased in neurons from TRPC5 KO mice (Fig. 10C). In addition, deficiency of TRPC5 had no effect on H_2O_2-triggered increases in $[Zn^{2+}]_i$ (Fig. 10D), indicating that TRPC5 does not mediate increases in Zn^{2+} during oxidative stress. Thus, these data provide that TRPC5 mediates H_2O_2-triggered Ca^{2+} influx into neurons, which is inhibited by NU6027 and I3O.

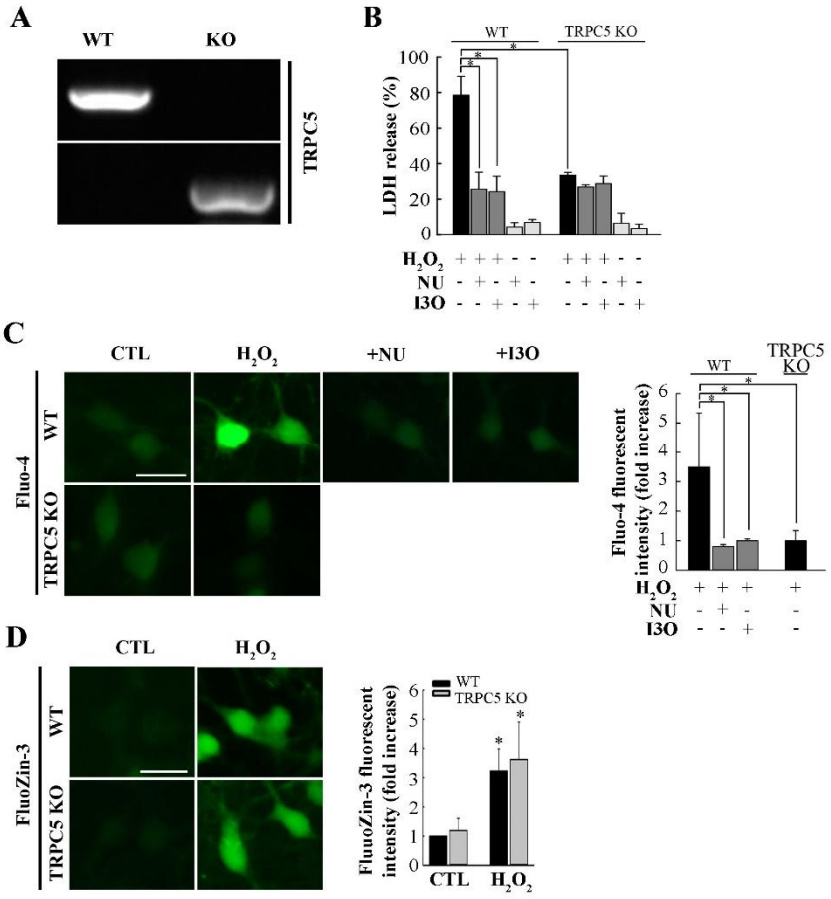

Fig. 10. H_2O_2-induced neuronal death and increases in $[Ca^{2+}]_i$ were diminished in neurons form TRPC5 KO mice. (A) Genetic ablation of TRPC5 was determined by PCR analysis. (B) Pure neuronal cultures from WT and TRPC5 KO littermate mice were exposed to 40 μM H_2O_2 for 24 h with or without NU6027 or I3O. The bars denote the percentage of LDH release (mean ± SEM, n = 3; ** indicates $p < 0.001$). (C) Pure neuronal cultures from WT and TRPC5 KO mice were exposed to 40 μM H_2O_2 for 2 h in the presence or absence of NU6027 and I3O and stained with Fluo-4 AM. The bar graphs represent the normalized fluorescence intensity of Fluo-4 AM (mean ± SEM, n = 3; * indicates $p < 0.05$). (D) Pure neuronal cultures from WT and TRPC5 KO mice were exposed to 40 μM H_2O_2 for 30 min and stained with FluoZin-3 AM. The bar graphs represent the normalized fluorescence intensity of FluoZin-3 (mean ± SEM, n = 3; * indicates $p < 0.05$).

NU6027 and I3O directly block both the basal activity and Zn^{2+}-mediated activation of TRPC5

To examine whether NU6027 and I3O directly block TRPC5 activity, electrophysiological recordings in HEK293 cells expressing mouse TRPC5 were performed. NU6027 or I3O almost completely blocked the increased basal current of TRPC5 induced by the addition of external Cs^{+}, which is highly permeable (Fig. 11A and B). To determine the effect of intracellular Zn^{2+} on TRPC5 activity, we infused with Zn^{2+} at varying concentrations. $Zn^{2+}$of ~5 μM half-maximally increased the basal inward Na^{+} current of TRPC5 (Fig. 12 A and B). The peak TRPC5 current induced by intracellular Zn^{2+} was also attenuated by NU6027 and I3O (Fig. 12C). These results support the possibility that NU6027 and I3O directly block TRPC5 at the resting state and Zn^{2+}- induced active state.

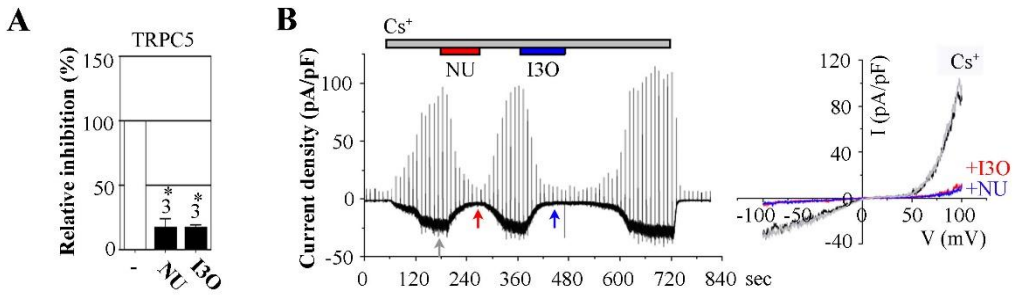

Fig. 11. NU6027 and I3O inhibited basal activity of TRPC5. (A) Inhibition of basal TRPC5 activity by treatment with 1 μM NU6027 or 10 μM I3O in HEK293 cells expressing TRPC5 (mean ± SEM, n = 3; * indicates $p < 0.05$ compared with control). (B) Representative current traces (left) and I–V curves (right) of basal TRPC5 activity and its inhibition by NU6027 and I3O.

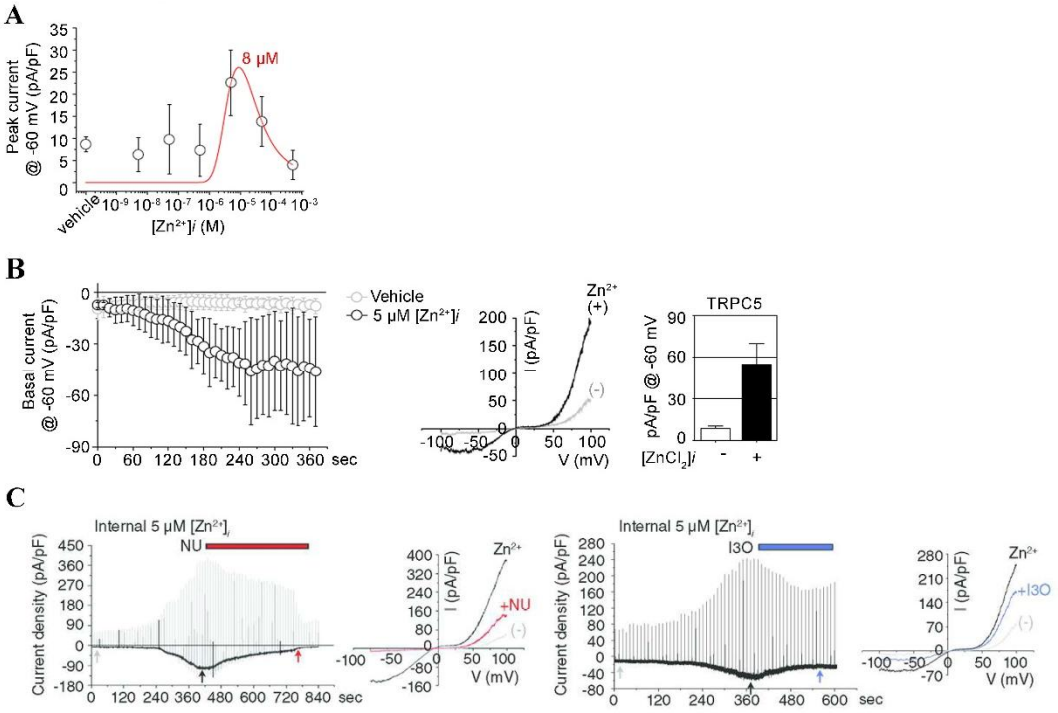

Fig. 12. NU6027 and I3O inhibited Zn^{2+}-activated TRPC5 currents. (A) Dose-dependent changes in TRPC5 activity caused by the intracellular application of Zn^{2+} in TRPC5-expressing HEK293 cells (mean ± SEM, n = 4). (B) Quantitative changes in basal inward Na^{+} currents (left) and I–V curves (middle) induced by intracellular 5 μM Zn^{2+} (mean ± SEM, Vehicle, n = 8; Zn^{2+}, n = 4). Changes in basal inward Na+ currents (right) induced by intracellular 5 μM Zn^{2+} (mean ± SEM, Vehicle, n = 8; Zn^{2+}, n = 4, ** indicates $p < 0.001$). (C) Representative current traces and I–V curves of intracellular Zn^{2+}-induced TRPC5 activation and its inhibition by NU6027 and I3O.

NU6027 prevents neuronal death in KA-injected rat seizure model

Finally, the protective effect of NU6027 was examined in KA-induced seizure animal model. The severity of seizure induced by KA within 2 h were not altered by the injection of NU6027 compare with vehicle-injected animals (Fig. 13 A), and the reduction of body weight was not recovered by NU6027 at 24 h after KA injection. However, the mortality 24 h after KA injection was markedly reduced in NU6027-injected animal (Fig. 13C). To determine the loss of cells, the brain sections were stained with cresyl violet. The result showed that the injection of NU6027 markedly diminished neuronal cell loss in CA1 and CA3, but less effective in piriform cortex (Pir), amygdala (Amg), (Fig. 14A). In addition to this, the brain sections were stained with Fluoro-Jade B (FJB) to assess the neuronal death. Consistent with neuronal loss, FJB-positive neurons were significantly reduced by the injection of NU6027 in Pir, Amg, CA1, and CA3. (Fig. 12B-D).

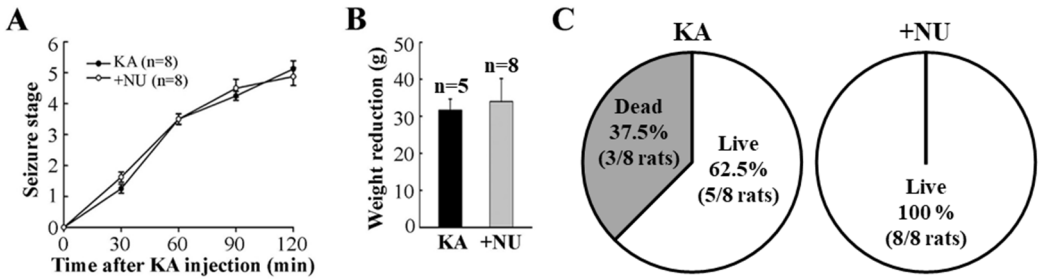

Fig. 13. NU6027 decreased mortality in kainic acid (KA)-induced seizure animal models. (A) Seizure stages were evaluated in SD rats injected with 10 mg/kg KA for 2 h (mean ± SEM, n = 8). Vehicle or 100 μg/kg NU6027 were injected 30 min after KA injection. (B) Bars denote the reduction of body weight 24 h after KA injection (mean ± SEM, KA, n = 5; NU, n = 8). (C) Mortality were determined 24 h after KA induction (mean ± SEM, KA, n = 8; NU, n = 8).

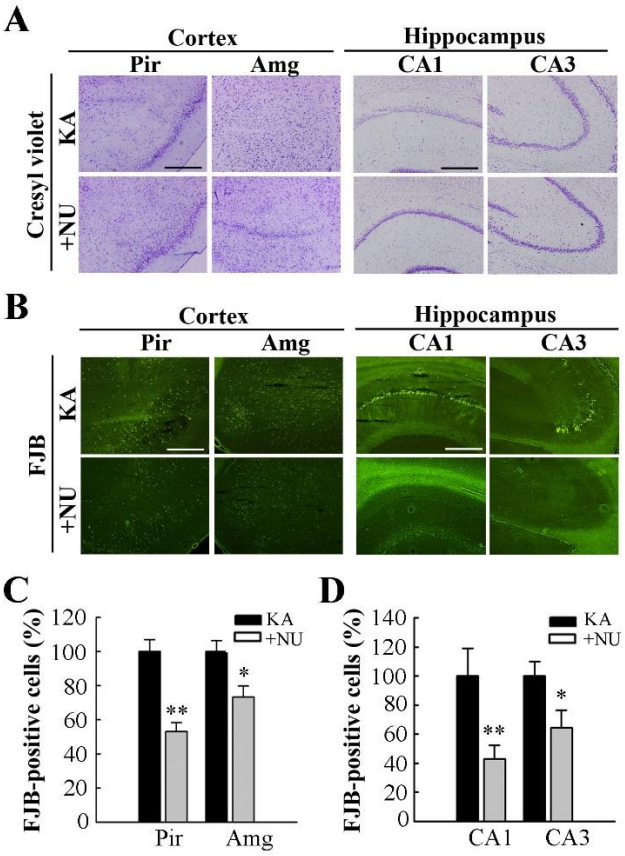

Fig. 14. NU6027 reduced KA-induced cell death in cortex and hippocampus. (A) Live neurons were stained with 1% cresyl violet. (B) Dead cells were stained with 0.001% FJB and observed under the fluorescent microscope. (C)The bar graphs represent the number of FJB-positive cells in the piriform cortex (Pir) and amygdala (Amg). (D) The bar graphs represent the number of FJB-positive cells in CA1 and CA3 regions of hippocampus (mean ± SEM, KA, n = 5; NU, n = 8, * indicates $p < 0.05$ and ** indicates $p < 0.001$ compared with KA).

Discussion

Increases in the $[Zn^{2+}]_i$ and $[Ca^{2+}]_i$ have been implicated to oxidative cell death in neuropathological conditions, such as ischemic brain injury, traumatic brain injury as well as epilepsy.[11, 22, 24, 25] However, the relationship between Ca^{2+} and Zn^{2+} has not been clearly studied under oxidative stress condition. Mechanisms involved in oxidative stress-induced neuronal cell death have been investigated intensively over the last several decades. During neuronal death induced by oxidative stress, $[Ca^{2+}]_i$ and $[Zn^{2+}]_i$ are excessively elevated and lead neuronal death in a various neurological disorders.[23, 43] Whereas Ca^{2+} overload has been discussed as a major ionic mechanism leading to cell death, more recently, Zn^{2+} dyshomeostasis has been proposed as an additional mechanism of neuronal death.[23,24] Under oxidative stress, Zn^{2+} binding proteins, such as metallothioneins, can release Zn^{2+} under oxidative conditions.[44,45] Prolonged Zn^{2+} dyshomeostasis can activate various cellular processes such as mitochondrial damage, NADPH oxidase activation, poly(ADP-ribose) polymerase activation, and lysosomal membrane permeabilization (LMP), which eventually lead to cell death.[46-48] However, the implications of these two ions on oxidative stress-induced neuronal death are not fully understood.

In this study, I found that H_2O_2 derived the early transient increases in $[Zn^{2+}]_i$ and delayed prolonged increases in $[Ca^{2+}]_i$ which contribute to the neuronal death. Addition of TPEN, a Zn^{2+}-specific chelator, completely blocks the increase in $[Ca^{2+}]_i$ induced by H_2O_2 while the treatment of TPEN after the peak of $[Zn^{2+}]_i$ did not blocked. This supports that the increase in free Zn^{2+} levels appears to be necessary prior to the delayed accumulation of Ca^{2+}, and that delayed and prolonged Ca^{2+} influx is likely the final cause of cell death induced by oxidative insults. The present study found that CDK inhibitors, NU6027 and I3O, are strong neuroprotective agents against oxidative stress-induced neuronal death and the increase in $[Ca^{2+}]_i$ while they did not block the increases in $[Zn^{2+}]_i$. This indicates that NU6027 and I3O may block the event involving the Ca^{2+} entry induced by oxidative stress. Therefore, this study

further analyzed the possible Ca^{2+} channels or receptors which mediate the Ca^{2+} influx.

Over the late several decades, the mechanisms of oxidative stress-induced neuronal death have been intensively studied. Abnormal elevation of Ca^{2+} is a one of the major factors for neuronal cell death.[11, 12] Although various receptors and channels are involving Ca^{2+} influx, TRP channels play important roles in oxidative stress-mediated neuronal death. The results in this study showed that the treatment with 2-APB, a broad-spectrum inhibitor of TRP channels, significantly prevented H_2O_2-induced neuronal death and increase in $[Ca^{2+}]_i$. This provides an evidence that TRP channels play a critical role on oxidative stress-induced neuronal death and increases in $[Ca^{2+}]_i$. Mammalian TRP channels are known as a Ca^{2+}-permeable non-selective cationic channels and divided into seven subfamilies. It has been suggested that TRPC, TRPM, and TRPV were involved in the oxidative stress-induced neuronal death.[17, 21, 36-38] There are several evidences, including capsaicin-triggered activation of TRPV1 in mesencephalic dopaminergic neuronal death,[39] amyloid β and H_2O_2-induced TRPM2 activation in striatal cell death,[14] and ROS-mediated TRPM7 activation in ischemic neuronal injury.[36] However, the results in this study found that non only the inhibitors for TRPM and TRPV did not prevent H_2O_2-induced neuronal death but also NU6027 and I3O had no effect on capsaicin-induced neuronal death and increases in $[Ca^{2+}]_i$. Interestingly, the results showed that ML204, an inhibitor for TRPC4 and TRPC5, markedly reduced neuronal death and the increase in $[Ca^{2+}]_i$ induced by H_2O_2. However, TRPC5 was exclusively expressed in neurons only while TRPC4 was expressed in both neurons and astrocytes. These data suggest that TRPC5 rather than TRPC4 may play a crucial role in Ca^{2+} influx in oxidative stress-induced neuronal death. Supportably, TRPC5 KO neurons are less vulnerable to oxidative stress compared with WT neurons. This results support that the elevation of $[Ca^{2+}]_i$ by H_2O_2 is due to the activation of TRPC5 rather than other TRP channels, such as TRPM and TRPV. Thus, this study provides the evidence that TRPC5 is critical in Ca^{2+} increases during oxidative stress-induced neuronal cell death.

One notable feature of TRP channels is that the activity and expression of TRP channels can be regulated by metal ions including Zn^{2+}. Previously, several studies reported that the increased in the intracellular Zn^{2+} induced the increases of the excitotoxic Ca^{2+} through the activation of TRPA in CA1 pyramidal neurons[28, 29] However, the implications of Zn^{2+}on TRPC5 activation are not fully understood. Therefore, the findings in this study demonstrated that Zn^{2+} directly participates in the activation of TRPC5 as in the case of TRPA1. Furthermore, the ablation of TRPC5 in neuron did not induced neuronal cell death and Ca^{2+} rises while $[Zn^{2+}]_i$ was maintained in higher levels. Although no detailed information regarding the gating mechanism for TRPC5 is yet available, this study suggests an intriguing possibility that Zn^{2+} contributes to the activation of TRPC5 induced by H_2O_2.

In addition, the present study noted that transient increases in the levels of Zn^{2+} play a prerequisite role for the delayed and prolonged Ca^{2+} influx. Hence, even increase in $[Zn^{2+}]_i$ is not severe enough to cause cell death, it may still play an important role in permitting the large influx of Ca^{2+} through TRPC5 during oxidative stress-induced neuronal death. Furthermore, the results indicated that NU6027 and I3O inhibited increases in $[Ca^{2+}]_i$, but they could not block the elevation of $[Zn^{2+}]_i$ induced by H_2O_2. This provides a possibility of that NU6027 and I3O may block TRPC5 activity. Electrophysiological results showed that NU6027 and I3O directly block not only the basal activity but also Zn^{2+}-mediated activation of TRPC5. This indicates that the protective effect of NU6027 and I3O against oxidative stress-induced neuronal death is associated with inhibition of TRPC5-mediated Ca^{2+} influx.

Epilepsy is one of the most common neurological disorders which are associated with oxidative stress.[8] Although current anti-epileptic drugs can control the seizure event in 70% patients, it still remains unavailable to control rest of the patients with epilepsy.[1] In cortical lesions of the focal cortical dysplasia, the expression of TRPC5 is increased in glutamatergic and GABAergic neurons.[2, 3] Furthermore, several lines of studies recently reported that TRPC5 play a critical role in epileptogenesis and neuronal death.[20, 21] Based on findings in

this study, NU6027 prevented neuronal death and blocked Zn^{2+}-induced TRPC5 activation resulting in Ca^{2+} influx. Therefore, NU6027 may effectively rescue the seizure-induced neuronal cell death. This study showed that NU6027, as a TRPC5 blocker, could not reduce KA-induced seizure severity. However, NU6027 significantly reduced seizure-induced neuronal cell death and mortality in KA-injected rats. Even though NU6027 cannot rescue the animals from seizure activity, these data suggest that NU6027 is a potent reagent to prevent neuronal death induced by epileptic seizures.

In conclusion, this study demonstrated that oxidative stress activates TRPC5 contributing Zn^{2+}-triggered delayed Ca^{2+} increases and that NU6027 and I3O block the in Ca^{2+} influx via directly inhibiting Zn^{2+}-mediated activation of TRPC5. Furthermore, animal study also identifies that NU6027 is a potent neuroprotective agent against neuronal death in KA-injected seizure animal model. All together this study strongly suggests that the inhibiting TRPC5 activity can be a possible therapeutic strategy for preventing neuronal death in epilepsy, even late stages.

References

1. Kwan P, Schachter SC, Brodie MJ. Drug-resistant epilepsy. N Engl J Med 2011;365:919-26.
2. Cavazos JE, Jones SM, Cross DJ. Sprouting and synaptic reorganization in the subiculum and CA1 region of the hippocampus in acute and chronic models of partial-onset epilepsy. Neuroscience 2004;126:677-88.
3. Gluck MR, Jayatilleke E, Shaw S, Rowan AJ, Haroutunian V. CNS oxidative stress associated with the kainic acid rodent model of experimental epilepsy. Epilepsy Res 2000;39:63-71.
4. Waldbaum S, Patel M. Mitochondrial dysfunction and oxidative stress: a contributing link to acquired epilepsy? J Bioenerg Biomembr 2010;42:449-55.
5. Cornelius C, Crupi R, Calabrese V, Graziano A, Milone P, Pennisi G, et al. Traumatic brain injury: oxidative stress and neuroprotection. Antioxid Redox Signal 2013;19:836-53.
6. Love S. Oxidative stress in brain ischemia. Brain Pathol 1999;9:119-31.
7. Uttara B, Singh AV, Zamboni P, Mahajan RT. Oxidative stress and neurodegenerative diseases: a review of upstream and downstream antioxidant therapeutic options. Curr Neuropharmacol 2009;7:65-74.
8. Shin EJ, Jeong JH, Chung YH, Kim WK, Ko KH, Bach JH, et al. Role of oxidative stress in epileptic seizures. Neurochem Int 2011;59:122-37.
9. Winyard PG, Moody CJ, Jacob C. Oxidative activation of antioxidant defence. Trends Biochem Sci 2005;30:453-61.
10. Floyd RA, Carney JM. Free radical damage to protein and DNA: mechanisms involved and relevant observations on brain undergoing oxidative stress. Ann Neurol 1992;32 Suppl:S22-7.

11. Berridge MJ. Neuronal calcium signaling. Neuron 1998;21:13-26.

12. Liu SJ, Zukin RS. Ca2+-permeable AMPA receptors in synaptic plasticity and neuronal death. Trends Neurosci 2007;30:126-34.

13. Ruiz A, Matute C, Alberdi E. Endoplasmic reticulum Ca(2+) release through ryanodine and IP(3) receptors contributes to neuronal excitotoxicity. Cell Calcium 2009;46:273-81.

14. Fonfria E, Marshall IC, Boyfield I, Skaper SD, Hughes JP, Owen DE, et al. Amyloid beta-peptide(1-42) and hydrogen peroxide-induced toxicity are mediated by TRPM2 in rat primary striatal cultures. J Neurochem 2005;95:715-23.

15. Hong C, Seo H, Kwak M, Jeon J, Jang J, Jeong EM, et al. Increased TRPC5 glutathionylation contributes to striatal neuron loss in Huntington's disease. Brain 2015;138:3030-47.

16. Clapham DE, Runnels LW, Strubing C. The TRP ion channel family. Nat Rev Neurosci 2001;2:387-96.

17. Miller BA. The role of TRP channels in oxidative stress-induced cell death. J Membr Biol 2006;209:31-41.

18. Nilius B, Szallasi A. Transient receptor potential channels as drug targets: from the science of basic research to the art of medicine. Pharmacol Rev 2014;66:676-814.

19. Strubing C, Krapivinsky G, Krapivinsky L, Clapham DE. TRPC1 and TRPC5 form a novel cation channel in mammalian brain. Neuron 2001;29:645-55.

20. Phelan KD, Mock MM, Kretz O, Shwe UT, Kozhemyakin M, Greenfield LJ, et al. Heteromeric canonical transient receptor potential 1 and 4 channels play a critical role in epileptiform burst firing and seizure-induced neurodegeneration. Mol Pharmacol 2012;81:384-92.

21. Phelan KD, Shwe UT, Abramowitz J, Wu H, Rhee SW, Howell MD, et al. Canonical transient receptor channel 5 (TRPC5) and TRPC1/4 contribute to seizure and

excitotoxicity by distinct cellular mechanisms. Mol Pharmacol 2013;83:429-38.

22. Frederickson CJ, Koh JY, Bush AI. The neurobiology of zinc in health and disease. Nat Rev Neurosci 2005;6:449-62.

23. Koh JY. Zinc and disease of the brain. Mol Neurobiol 2001;24:99-106.

24. Sensi SL, Paoletti P, Bush AI, Sekler I. Zinc in the physiology and pathology of the CNS. Nat Rev Neurosci 2009;10:780-91.

25. Koh JY, Suh SW, Gwag BJ, He YY, Hsu CY, Choi DW. The role of zinc in selective neuronal death after transient global cerebral ischemia. Science 1996;272:1013-6.

26. Suh SW, Chen JW, Motamedi M, Bell B, Listiak K, Pons NF, et al. Evidence that synaptically-released zinc contributes to neuronal injury after traumatic brain injury. Brain Res 2000;852:268-73.

27. Buhl EH, Otis TS, Mody I. Zinc-induced collapse of augmented inhibition by GABA in a temporal lobe epilepsy model. Science 1996;271:369-73.

28. Vander Jagt TA, Connor JA, Weiss JH, Shuttleworth CW. Intracellular Zn2+ increases contribute to the progression of excitotoxic Ca2+ increases in apical dendrites of CA1 pyramidal neurons. Neuroscience 2009;159:104-14.

29. Andersson DA, Gentry C, Moss S, Bevan S. Clioquinol and pyrithione activate TRPA1 by increasing intracellular Zn2+. Proc Natl Acad Sci U S A 2009;106:8374-9.

30. Proctor PH, Tamborello LP. SAINT-I worked, but the neuroprotectant is not NXY-059. Stroke 2007;38:e109; author reply e10.

31. Bavarsad Shahripour R, Harrigan MR, Alexandrov AV. N-acetylcysteine (NAC) in neurological disorders: mechanisms of action and therapeutic opportunities. Brain Behav 2014;4:108-22.

32. Amaro S, Chamorro A. Translational stroke research of the combination of thrombolysis and antioxidant therapy. Stroke 2011;42:1495-9.

33. Zhang X, Gelowitz DL, Lai CT, Boulton AA, Yu PH. Gradation of kainic acid-induced

rat limbic seizures and expression of hippocampal heat shock protein-70. Eur J Neurosci 1997;9:760-9.

34. Chuang DM, Wang Z, Chiu CT. GSK-3 as a Target for Lithium-Induced Neuroprotection Against Excitotoxicity in Neuronal Cultures and Animal Models of Ischemic Stroke. Front Mol Neurosci 2011;4:15.

35. Cohen P, Goedert M. GSK3 inhibitors: development and therapeutic potential. Nat Rev Drug Discov 2004;3:479-87.

36. Aarts M, Iihara K, Wei WL, Xiong ZG, Arundine M, Cerwinski W, et al. A key role for TRPM7 channels in anoxic neuronal death. Cell 2003;115:863-77.

37. Flockerzi V, Nilius B. TRPs: truly remarkable proteins. Handb Exp Pharmacol 2014;222:1-12.

38. Nagarajan A, Ning Y, Reisner K, Buraei Z, Larsen JP, Hobert O, et al. Progressive degeneration of dopaminergic neurons through TRP channel-induced cell death. J Neurosci 2014;34:5738-46.

39. Kim SR, Lee DY, Chung ES, Oh UT, Kim SU, Jin BK. Transient receptor potential vanilloid subtype 1 mediates cell death of mesencephalic dopaminergic neurons in vivo and in vitro. J Neurosci 2005;25:662-71.

40. Riccio A, Li Y, Moon J, Kim KS, Smith KS, Rudolph U, et al. Essential role for TRPC5 in amygdala function and fear-related behavior. Cell 2009;137:761-72.

41. Lau OC, Shen B, Wong CO, Tjong YW, Lo CY, Wang HC, et al. TRPC5 channels participate in pressure-sensing in aortic baroreceptors. Nat Commun 2016;7:11947.

42. Ma X, Cai Y, He D, Zou C, Zhang P, Lo CY, et al. Transient receptor potential channel TRPC5 is essential for P-glycoprotein induction in drug-resistant cancer cells. Proc Natl Acad Sci U S A 2012;109:16282-7.

43. Choi DW. Calcium and excitotoxic neuronal injury. Ann N Y Acad Sci 1994;747:162-71.

44. Aizenman E, Stout AK, Hartnett KA, Dineley KE, McLaughlin B, Reynolds IJ. Induction of neuronal apoptosis by thiol oxidation: putative role of intracellular zinc release. J Neurochem 2000;75:1878-88.

45. Lee JY, Cho E, Kim TY, Kim DK, Palmiter RD, Volitakis I, et al. Apolipoprotein E ablation decreases synaptic vesicular zinc in the brain. Biometals 2010;23:1085-95.

46. Hwang JJ, Lee SJ, Kim TY, Cho JH, Koh JY. Zinc and 4-hydroxy-2-nonenal mediate lysosomal membrane permeabilization induced by H_2O_2 in cultured hippocampal neurons. J Neurosci 2008;28:3114-22.

47. Kim YH, Koh JY. The role of NADPH oxidase and neuronal nitric oxide synthase in zinc-induced poly(ADP-ribose) polymerase activation and cell death in cortical culture. Exp Neurol 2002;177:407-18.

48. Noh KM, Kim YH, Koh JY. Mediation by membrane protein kinase C of zinc-induced oxidative neuronal injury in mouse cortical cultures. J Neurochem 1999;72:1609-16.

국문 초록

배경: 뇌전증은 반복적 인 자연 발작과 이로 인한 신경 세포 죽음이 일어나는 가장 흔한 신경 질환 중 하나이다. 중추 신경계의 신경 세포는 발작, 허혈성 뇌 손상 및 외상성 뇌 손상과 같은 급성 뇌 손상에서 종종 발생하는 산화 스트레스에 매우 취약하다. 산화적 신경 손상 동안, 세포 내 칼슘 이온(Ca^{2+})과 아연 이온(Zn^{2+})은 과도하게 증가되며, 이들은 신경 세포 사멸에서 매우 중요한 역할을 수행하나, 신경세포 사멸에서의 산화적 손상의 명확한 기전과 이들 두 이온의 역할에 대한 규명이 잘 밝혀져 있지 않아 연구가 필요하다.

목적: 본 연구의 목적은 산화 스트레스에 의해 유발 된 신경 세포 죽음에 대한 강력한 신경 보호 물질을 발굴하고, 이들 물질들의 신경 보호 효과에 대한 메커니즘을 규명하고, 산화 스트레스에 의해 유발 된 Ca^{2+} 유입 경로 및 Zn^{2+}와의 연관성을 규명하는 것이다.

결과: 대뇌 피질 뉴런과 성상교세포 모두를 포함하는 일차 배양체를 H_2O_2에 노출시켰을 때, 대다수의 세포가 죽으면서 배양중인 배지로 lactose dehydrogenase (LDH)의 분비가 증가하였다. NU6027 또는 indirubin-3'-oxime (I3O)의 첨가는 H_2O_2에 의해 유도 된 세포 사멸을 현저히 감소시켰다. 또한, NU6027 또는 I3O 는 $ZnCl_2$ 또는 SNP(산화 질소 공여자) 처리로 유도된 세포사도 억제하였다. 흥미롭게도 이들 약물의 보호 효과는 신경세포에 특이 적이었으며 성상교세포 사멸은 전혀 억제하지 못하였다. Live cell imaging을 이용하여 H_2O_2에 노출 된 신경세포에서의 Zn^{2+} 및 Ca^{2+} 분석한 결과, Zn^{2+} 증가는 매우 빠르게 일어나고 Ca^{2+} 증가는 그 이후 일어나며, NU6027 또는 I3O는 H_2O_2에 의한 세포 내 Zn^{2+} 증가에는 영향을 주지 못했지만, Ca^{2+} 증가는 효과적으로 억제 하였다. 반면, TPEN은 H_2O_2에 의한 Zn^{2+}와 Ca^{2+} 증가를 모두 억제 하는 것을 확인 하였다. 이러한 결과는 초기

Zn^{2+} 증가가 후기 Ca^{2+} 증가 전제조건임을 보여준다. H_2O_2에 의해 유발된 세포 사멸의 원인이 되는 Ca^{2+} 유입 경로를 알아 내기 위해, Ca^{2+} 유입과 관련된 수용체 및 채널에 대한 억제제를 처리하였다. 사용한 억제제 중 NMDA, CNQX, XeC, dantrolene의 경우 H_2O_2에 의해 유발 된 신경 세포 사멸을 억제하지 못하였으나, 2-APB와 ML204는 H_2O_2에 의해 유발 된 신경 세포 사멸을 억제할 뿐만 아니라 Ca^{2+} 증가를 매우 효과적으로 감소 시켰다. 이는 transient receptor potential canonical 5 (TRPC5)가 Ca^{2+} 증가와 신경 세포 사멸에 관여 될 수 있음을 시사한다. 또한, TRPC 채널 중 TRPC5가 뉴런에서만 특이적으로 발현 되는 것을 확인하였으며, TRPC5 knock out (KO) 마우스의 신경세포 배양체는 H_2O_2에 의한 신경세포 사멸에 내성을 보였다. 마우스 TRPC5 단백질을 발현하는 HEK293 세포를 이용한 전기 생리학적 실험에서 NU6027 및 I30가 TRPC5 활성 및 Zn^{2+}에 의한 TRPC5 활성화를 직접적으로 차단함을 보여 주었다. 마지막으로, kainic acid(KA)에 의한 발작 백서 모델에서 NU6027은 발작의 정도를 억제 하지는 못하였으나, 사망률과 대뇌 피질과 해마 영역에서 신경 세포 사멸을 현저하게 감소시켰다.

결론: NU6027과 I30는 산화 스트레스에 의해 유도되는 아연 의존적 독성 Ca^{2+} 유입을 매개하는 TRPC5 활성을 직접적으로 억제하였다. 따라서, TRPC5 활성 저해는 뇌전증에 대한 약물 개발을 위한 새로운 타겟이 될 수 있다.

핵심단어: Transient receptor potential canonical 5 (TRPC5), 뇌전증, 산화적 손상, 신경 세포 사멸, 아연 이온, 칼슘 이온